Engineering Structures 269 (2022) 114810

Contents lists available at ScienceDirect

Engineering Structures

journal homepage: www.elsevier.com/locate/engstruct

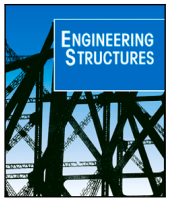

Statistical correlation investigation of a single-doweled timber-to-timber joint

Caroline D. Aquino [a,*], Leonardo G. Rodrigues [a], Jorge M. Branco [a], Wellison J.S. Gomes [b]

[a] Institute for Sustainability and Innovation in Structural Engineering (ISISE), University of Minho, Guimarães, Portugal
[b] Center for Optimization and Reliability in Engineering (CORE), Department of Civil Engineering, Federal University of Santa Catarina, Florianópolis, SC, Brazil

ARTICLE INFO

Keywords:
Timber joints
Uncertainty quantification
Joint behavior
Copula theory
Reliability analysis

ABSTRACT

Dowel-type joints are widely used in timber structures given their ease of construction, strength, and capacity to deform before failure. The embedment strength of timber and the bending moment capacity of dowels are considered key properties in the design. On the other hand, these properties have an inherent variability that increases the uncertainties related to the connection's strength and associated failure modes. This study proposes to quantify the uncertainty related to the statistical correlation behavior between the timber embedment strength and dowel bending moment capacity while comparing analytical solutions to the results of double shear single doweled timber joints. Traditional distribution fitting procedures, as well as copula functions, are implemented to capture their marginal and dependence behavior. Since their source of mutual correlation is known, the effectiveness of the different approaches in describing the statistical dependence structure can be assessed. This is done by investigating how equivalent are the descriptions of dependence by copula functions and directly from the correlation origin. Results obtained here indicate that, for single dowel-type connections in double shear, the impact of the copulas on the results is small, which means that improving their joint characterization represents a minor improvement in the reliability results. Besides the minor differences, the results show that copula functions are a viable tool capable of capturing the nuances of the joint behavior between random variables.

1. Introduction

The design of connections has long been identified as the most critical part of the design phase of a timber structure [1]. In fact, it is crucial to assess the efficiency of connections due to their impact on the overall structural strength and stiffness, compliance with distinct serviceability limit states and fire resistance [2]. Moreover, the assessments of severely damaged timber structures under extreme loading frequently point out the inadequacy of the connections as the main cause of failure [3–5]. Thus, it becomes essential to perform studies on the behavior of connections, to better understand them and to provide adequate guidelines for their design.

The inherent variability of timber, as well as its impact on the safety of structural members, is relatively well understood and has been addressed in the literature (e.g., [6–8]). However, only a few researchers performed reliability assessments of timber connections with dowel-type fasteners [2,9], as well as data characterization of the parameters involved in their design [10–12]. Indeed, the application of structural reliability methods has led to an increasingly more consistent safety evaluation of structural elements and of the overall capacity of structures [13,14].

Köhler [2] proposed a probabilistic framework for the reliability assessment of dowel-type connections, considering the timber density and the steel yield capacity in tension as the resistance random variables. The connection resistance was weighted by a model uncertainty parameter, which proved to be of great relative importance to the probability of failure. Later, Jockwer, Fink, and Köhler [9] addressed the assessment of the failure behavior and reliability of timber connections with multiple dowel-type fasteners, where the occurrence of brittle failure modes was considered. The fracture energies associated to splitting and block shear were considered as random variables. They concluded that the variability of the load carrying capacity depends not only on the material variability but also on the respective failure mode prone to occur. In general, failure modes with a brittle failure mechanism lead to a higher variability compared to ductile failure mechanisms, as expected.

* Corresponding author.
E-mail addresses: carolinedapieve@gmail.com (C.D. Aquino), leonardofgrodrigues@gmail.com (L.G. Rodrigues), jbranco@civil.uminho.pt (J.M. Branco), wellison.gomes@ufsc.br (W.J.S. Gomes).

https://doi.org/10.1016/j.engstruct.2022.114810
Received 21 June 2021; Received in revised form 11 July 2022; Accepted 7 August 2022
Available online 20 August 2022

Despite the efforts made towards a wide use of reliability analysis, the developments reached so far have had less impact for the design of timber structures than the impact observed for structures built with other common materials, such as concrete and steel [7,15]. According to the specialized literature, most of the efforts spent in the field of structural reliability have been focused especially on the improvement of methods to assess the probability of failure (e.g., [16–18]). However, it has been noted that an adequate description of the input data has more impact towards better estimations of the structural reliability than the precision of the available methods to assess it [19].

Therefore, recent studies (e.g., [19–21]) gave special attention to input data characterization, aiming to improve the robustness of the reliability analysis. A better description of the statistical correlation between variables is required for structural reliability applications, as pointed out by Torre et al. [19]. In this regard, the Copula theory may be used to capture the dependence structure, and allows obtaining joint distributions by separately looking at the dependence and at the marginal behaviors.

Long-established reliability methods commonly adopt the Nataf transformation (see [22,23]) to include the linear correlation of data, which, according to Lebrun and Dutfoy [24], is equivalent to a Gaussian copula correlation construction. However, Wang and Li [21] pointed out that the implicit Gaussian dependence structure assumed may not be valid and bias the reliability results. In fact, Torre et al. [19] stated that in a scenario where the true statistical correlation among the variables is non-linear, assuming independence or a Gaussian correlation may cause severe misestimation of the failure probability.

Although there are other probabilistic methodologies that have been gaining wide acceptance in the literature [25–28], including those based on the classical Weibull Theory, which allows to take into account the size-effects related to the strength properties, the present paper focuses on the use of copulas. Copula theory is not new, but has been applied in many papers related to structural reliability in the last years [19,29,30], especially because it allows to capture possible non-linearity in the correlated behavior between random variables.

The present study aims to quantify the uncertainties associated to two strength properties that commonly govern the structural design of dowel-type timber connections. Namely, the timber embedment strength (f_h) and the bending moment capacity of the dowel (M_y). According to Blass et al. [31], these parameters are both related to the timber density (ρ) and are, consequently, correlated. Based on this premise, a correlation model is proposed in order to capture the dependence between the timber embedment strength and the dowel bending moment capacity. The effectiveness of the statistical dependence models employed herein is evaluated by comparing analytical and experimental results.

As far as it comes to the authors concern, the influence of the statistical correlation between f_h and M_y on the reliability assessment of timber connections has not been addressed in the literature yet. Moreover, when correlation is considered among other variables, it is usually addressed in terms of linear pair-wise correlation coefficients. Thus, the potentiality of nonlinear correlation models presented in this study constitutes an important development on the reliability evaluation of timber structural systems.

The paper is laid out as follows. In Section 2, some basic concepts related to the design of dowel-type timber joints are presented. In Section 3, the experimental campaign conducted to describe important variables related to the connection and respective results are presented. Section 4 describes statistical data modeling involving marginal and correlation inference according to the Copula theory. In Section 5, general concepts related to structural reliability are given, followed by the presentation of simple and importance sampling Monte Carlo methods. The methods differ from their traditional formats since they incorporate the dependence structure of the random variables written in terms of copula functions. Section 6 introduces the statistical dependence investigation from a theoretical point of view and presents the procedures adopted to the application on dowel-type timber joints. The data obtained from the experimental campaign is used for the statistical inference of the random variables involved in the reliability problem, which is given in Section 7. Finally, Section 8 presents results for application problems, involving the comparison between correlation models and different member thickness. Concluding remarks are presented in Section 9.

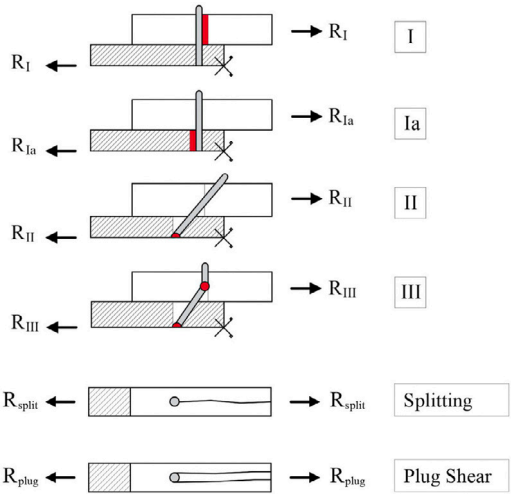

Fig. 1. Failure modes for timber-to-timber dowel-type joints in double shear.

2. Dowel-type timber joints

Dowel-type joints are frequently used in timber constructions due to their straightforward installation and effectiveness in terms of load-carrying capacity. However, an efficient design requires an adequate knowledge of their response, which is dependent of the geometry, load direction, and mechanical properties of timber and dowel material [32]. For example, the embedment strength of timber is strongly related to its density, which can vary considerably for distinct wood species [33,34]. On the other hand, the yield moment of the fastener is dependent of its diameter and steel grade. Moreover, the ratio between the member thicknesses and the diameter of the dowel, the so-called dowel slenderness, can be used to ensure failure modes that comply with predefined performance design objectives [35].

The main failure modes of a double shear single doweled joint loaded perpendicular to the fastener axis are represented in Fig. 1 for a symmetric half of the joint (front view). Mode I and mode Ia correspond to the embedment failures of the side, and middle member, respectively. The subsequent failure modes are characterized by the formation of a single plastic hinge (mode II) or two plastic hinges (mode III) in the dowel. Also contained in the figure are the modes related to brittle failure (lateral view), which according to Schmid et al. [36] will be either splitting or plug shear for this type of connection.

The load carrying capacity (R) per shear plane, associated to the ductile failure modes, can be obtained by the Johansen's yield theory [37], as follows:

$$R_I = f_{h,1} \cdot t_1 \cdot d \tag{1a}$$

$$R_{Ia} = 0.5 \cdot f_{h,2} \cdot t_2 \cdot d \tag{1b}$$

$$R_{II} = \frac{f_{h,1} \cdot t_1 \cdot d}{2+\chi}\left[\sqrt{2\chi(1+\chi)+\frac{4\chi(2+\chi)\cdot M_y}{f_{h,1}\cdot d\cdot t_1^2}}-\chi\right] \tag{1c}$$

$$R_{III} = \sqrt{\frac{2\chi}{1+\chi}}\sqrt{2\cdot M_y \cdot f_{h,1}\cdot d} \tag{1d}$$

where t_1 and t_2 are the thickness of the side member and middle member; $f_{h,1}$ and $f_{h,2}$ are the corresponding embedment strength of the side member and middle member; $\chi = f_{h,2}/f_{h,1}$ is the ratio between the embedment strength of the members; d is the fastener diameter; and M_y is the fastener yield moment.

The expressions derived by Johansen [37] for the load carrying capacity R are based on equilibrium conditions for each failure mode and assumed a symmetric connection. It is worth noting that the Eqs. (1c)–(1d) related to failure modes II and III do not consider the effect of friction along the dowel axis, neither the rope effect associated to the withdrawal capacity of the dowel.

Due to perpendicular to grain stresses that arise from dowel wedge into the wood, splitting or plug shear may arise [38]. International standards have set ground rules to prevent these failure modes by limiting the minimum fastener spacing, end-distances, and edge-distances. However, recent studies have shown that timber joints, designed according to Eurocode 5 provisions, may present brittle failures and low ductility [39,40].

Different analytical models exist in the literature to deal with splitting and plug shear. For instance, Jorissen [35] presented a fracture mechanics-based design approach for brittle failure of a connection, where the fracture process is described by a mixed mode fracture. Jensen and Quenneville [41] developed a model for plug shear using also the principles of fracture mechanics. Jockwer, Fink, and Köhler [9] proposed a simplified model that considers splitting as a consequence of the tensile stresses perpendicular to the grain. Yurrita and Cabrero [42] propose a similar approach, differing on the computation of the effective area where the perpendicular to the grain tensile stress is applied.

Nonetheless, brittle failure modes do not play a significant role in the scope of the present investigation since the interest is on the statistical correlation behavior between the timber embedment strength and effective bending moment, which are inherent properties of the ductile failure modes discussed herein. The experimental campaign conducted supports this approach; additional details regarding brittle failures are provided in Section 3.

2.1. Embedment strength

The embedment strength is the resistance of a timber element against the lateral penetration of a fastener. Its value is mostly influenced by the angle between the load and the grain direction, the density of wood and its moisture content, as well as the diameter of the fastener [43]. In the scope of the present paper, only connections loaded parallel to the grain are evaluated. The researches presented in [44–46] are in the basis of Eq. (2), given in Eurocode 5 (EC5) [47] for the parallel-to-grain embedment strength:

$$f_{h,0} = 0.082(1 - 0.01d)\rho \tag{2}$$

where d is the diameter of the fastener, in mm, and ρ is the density of timber, in kg/m^3, at a moisture content of 12%. From Eq. (2), one can conclude that elements with higher density present higher embedment strength, while an increment in the dowel diameter leads to lower values. Despite not being considered directly in Eq. (2), an increment of moisture content reduces the embedment strength of the timber members [11,33].

According to Glišović et al. [48], Eq. (2) presents good results for most of the European softwood species. However, there are some deviations for timber species with higher densities ($\rho \geq 500$ kg/m^3). Sandhaas et al. [11] performed embedment tests with five different wood species, among which three are tropical hardwood species, one is a European softwood and the other is a European hardwood. Based on the experimental results, they concluded that the EC5 embedment strength equation penalized wood species with higher densities. In turn, it overestimates the embedment strength of species characterized by having low densities. This statement is supported by Leijten et al. [10], which involves a considerable amount of experimental data, including those presented in [49,50]. A probabilistic analysis allowed the authors to propose distinct equations for softwoods and hardwoods, as follows:

$$f_{h,0} = 0.097 \cdot \rho^{1.07} \cdot d^{-0.25} \quad \text{for softwoods} \tag{3a}$$

$$f_{h,0} = 0.087 \cdot \rho^{1.09} \cdot d^{-0.25} \quad \text{for hardwoods} \tag{3b}$$

Other studies have proposed other parameters and equations for different wood species. Based on Franke and Quenneville [51], the revision of the New Zealand structural design code NZS3603 includes expressions for the embedment strength of Radiata pine (*Pinus radiata*), while Eq. (2) is still recommended for other species. In addition, the National Design Specification (NDS) [52] for Wood Construction proposes a different equation for North American softwoods, where the embedment strength is dependent only from wood density.

Tuhkanen et al. [53] studied the embedment strength of glulam members and evaluated the influence of the number of layers. From the experimental results obtained, Tuhkanen et al. [53] concluded that specimens with more layers are less prone to splitting failures, which can be related to the reinforcement of the adhesive layer. In addition, the authors stated that no size effect was detected due to different layer thicknesses.

In this paper, the timber embedment strength is assessed for glulam timber members of a European softwood species, where the EC5 model (2) is employed. This choice is supported by Glišović et al. [48] and Tuhkanen et al. [53]; they concluded that massive and glulam timber elements of European softwoods show good agreement with Eq. (2).

2.2. Bending moment capacity of the dowel

The bending moment capacity is the resistance of a dowel against bending. It is mainly influenced by the dowel diameter (d) and the yield strength (f_y) of the dowel material. In the scope of this paper, smooth dowels are considered made of mild steel. In the failure modes associated to plastic deformations of dowels, where their bending capacity is mobilized, the bending moment directly influences the load-carrying capacity of the connection. In terms of experimental evaluation, the characterization of the bending moment can be performed through a four-point bending test, according to the guidelines of EN 409 [54]. In the experiment, the yield moment of a fastener is determined at a bending angle of 45°. In this configuration, the whole cross-section of the dowel is assumed to be under plastic strain [31].

However, it is argued that when bolted connections are tested, and the failure modes achieved are characterized by the dowel's bent, the bending angles often lie below 45° (see [35]). In this scenario, the plastic capacity of the dowels is only partially used. The effective bending moment resides between the elastic ($M_{y,el} = 0.8 \cdot f_u \cdot \pi d^3/32$) and plastic ($M_{y,pl} = 0.8 \cdot f_u \cdot d^3/6$) bending capacity of the dowels' cross-section, considerably lower than the results achieved through EN 409 [54]. Here, f_u is the fastener tensile strength.

Blass et al. [31] proposed a penalty term in terms of the bending angle ($\bar{M}(\alpha)$) to address this partially mobilized plastic moment. The effective bending moment ($M_{y,eff}(\alpha)$) is given by the product between the plastic bending capacity $M_{y,pl} = M(\alpha = 45°)$ and the factor $\overline{M}(\alpha)$ (see Eqs. (4) and (5)).

$$\overline{M}(\alpha) = (0.866 + 0.00295\alpha)\left(1 - \exp\left(\frac{-0.248\alpha}{0.866}\right)\right) \tag{4}$$

$$M_{y,eff}(\alpha) = \overline{M}(\alpha) M(\alpha = 45°) \tag{5}$$

Therefore, to calculate the effective bending moment, one must know α. The bending angle can be measured directly from the load-carrying experiments, or through a theoretical approach presented by Blass et al. [31]. The expressions to assess α are derived from

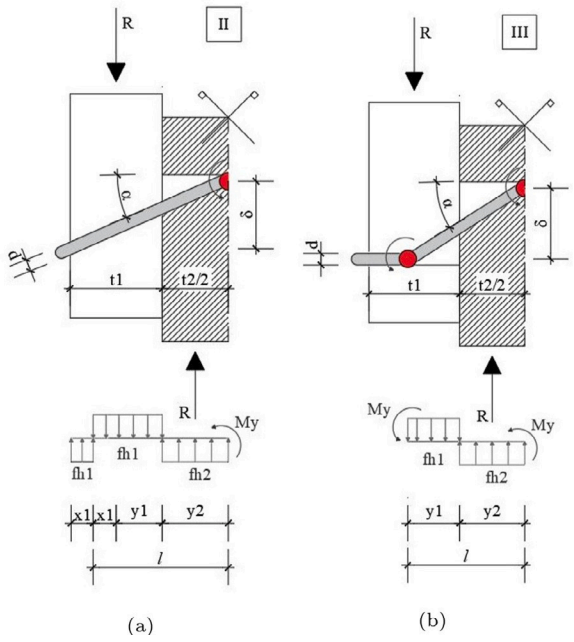

Fig. 2. Dowels' bent in double shear connections for (a) failure mode II, and (b) failure mode III.

equilibrium conditions. A scheme of the connection acting forces is given in Fig. 2, considering the symmetry of the problem.

From Fig. 2, α can be written in the format of $\alpha = \arctan\frac{\delta}{l}$. Where δ is the maximum deformation ($\delta = 15$ mm according to the guidelines of EN 26891 [55]); and l is the length where the embedment strength is reached. Obtaining the geometry variables x_1, y_1, and y_2 from equilibrium conditions (see [35]), α can be determined from Eq. (6) for failure mode II.

$$\alpha = \arctan\left(\frac{\delta}{\frac{t_1}{2} + \frac{t_1}{2+\chi}[a]\left(\frac{1}{2}+\chi\right)}\right), \quad \text{where}$$
$$a = \sqrt{2\chi(1+\chi) + \frac{4\chi(2+\chi)\cdot M_{y,eff}}{f_{h,1}\cdot d\cdot t_1^2}} - \chi \tag{6}$$

According to (6), α depends on $M_{y,eff}$. The dependence between these variables can be taken into account by an iterative procedure using Eq. (7). A first estimation is taken as $\alpha = 45°$. Subsequently, the $\overline{M}(\alpha)$ factor obtained in Eq. (4) is used in (7). The theoretical angle α usually converges after three iteration stpdf [31]. Once α is determined, the effective bending moment ($M_{y,eff}$) can be calculated by means of (5).

$$\alpha_{i+1} = \arctan\left(\frac{\delta}{\frac{t_1}{2} + \frac{t_1}{2+\chi}[a_{i+1}]\left(\frac{1}{2}+\chi\right)}\right), \quad \text{where}$$
$$a_{i+1} = \sqrt{2\chi(1+\chi) + \frac{4\chi(2+\chi)\cdot M(\alpha=45°)\cdot \overline{M}(\alpha_i)}{f_{h,1}\cdot d\cdot t_1^2}} - \chi \tag{7}$$

The same procedure can be used to derive the expressions for α for failure mode III, such expressions are presented in Eqs. (8) and (9).

$$\alpha = \arctan\left(\frac{\delta}{\sqrt{\frac{2\cdot\chi}{1+\chi}}\frac{\sqrt{2\cdot M_{y,eff}\cdot f_{h,1}\cdot d}}{f_{h,1}\cdot d}(1+\chi)}\right) \tag{8}$$

$$\alpha_{i+1} = \arctan\left(\frac{\delta}{\sqrt{\frac{2\cdot\chi}{1+\chi}}\frac{\sqrt{2\cdot M(\alpha=45°)\cdot \overline{M}(\alpha_i)\cdot f_{h,1}\cdot d}}{f_{h,1}\cdot d}(1+\chi)}\right) \tag{9}$$

Since larger values of the tensile strength and lower values of the density lead to significantly low values of α, Blass et al. [31] argues that governing parameters can be conservatively chosen, resulting in maximum values for the steel tensile strength and minimum values for the characteristic density. The authors show that when assuming $f_{u,k} = 1000$ N/mm^2 and $\rho_k = 350$ kg/m^3 their approach results in a similar format of Eq. (10). This equation is based on the work of Werner and Siebert [56], and consists in the analytical model presented by EC5 to assess the effective bending moment of nails, bolts, and dowels.

$$M_{y,eff} = 0.3\cdot f_u\cdot d^{2.6} \tag{10}$$

Comparing the results obtained from (10) with (5) for different values of the wood density, one can easily note that the calculations proposed in [31] are similar to the design guidelines for smaller dowels' diameter, however, the differences between approaches begin to increase for $d \geq 12$ mm. Blass and Colling [57] proposed a modified version of Eq. (10) based on an extensive database, given by Eq. (11), which considers that the bending angle, α, is dependent on the wood density, ρ. This equation was later validated by Sandhaas and Görlacher [58] for nailed connections.

$$M_{y,eff} = \frac{1}{6} f_{y,eff}\cdot d^3 \tag{11}$$

where:

$$f_{y,eff} = \begin{cases} \frac{0.9(f_y+f_u)}{2} & \text{for } f_u < 450 \text{ MPa} \\ 0.9 f_u & \text{for } f_u > 450 \text{ MPa} \end{cases} \tag{12}$$

Nonetheless, the formulation presented in Blass et al. [31] is adopted herein due to its generality. Moreover, it relates $M_{y,eff}$ with ρ, which is important to the statistical dependence investigation proposed herein.

3. Experimental campaign

An experimental campaign has been conducted at the University of Minho in Portugal to obtain information regarding some variables related to the connection. The campaign was divided into monotonic tests of double-shear and tensile tests of the steel fastener. The experiments and respective results are presented next.

3.1. Monotonic tests of double-shear connections

The load-carrying of double-shear timber-to-timber connections, loaded parallel to the grain, was evaluated by experimental tests, following the EN 26891 [55]. The test apparatus was designed to restrain rotations on two perpendicular test planes, through the use of two bracing frames attached to the base plate. The test setup, presented in Fig. 3, had a hydraulic actuator, equipped with a load cell of 100 kN, and a displacement range of 200 mm. In order to measure the joint slip, two LVDTs were fixed on both sides of the connection. These two LVDTs were placed diagonally opposing relatively to the central timber member. The first part of the testing load protocol consists of a loading branch, which is followed by a plateau, where the load is kept constant and equal to 40% of the estimated capacity during 30 s. After, the load is diminished until it reaches 10% of the estimated capacity and then kept constant for another 30 s. Thereafter, the test was performed under displacement control with a constant rate of 0.025 mm/s. Both loading and unloading branches are force controlled with a constant rate of 0.058 kN/s. The estimated load-carrying capacity ($F_{est} = 16.3$ kN) was determined by the lower value given by the Eqs. (1a)–(1d), based on the

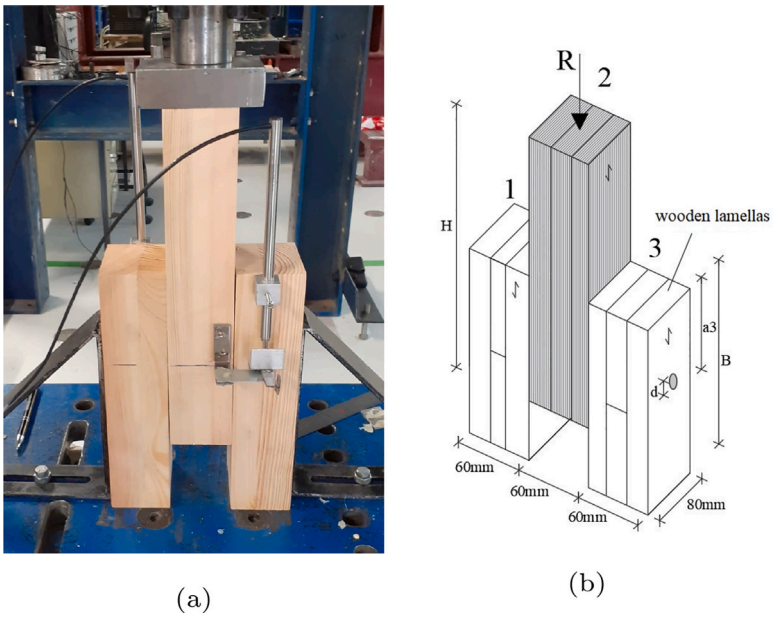

Fig. 3. Test setup according to EN 26891 [55]: (a) test apparatus, and (b) test scheme.

mean value of the density (420 kg/m^3), which is required to estimate the embedment strength, as well as the tensile strength of 360 N/mm^2 that is recommended by the supplier of the dowels. In the scope of the present paper, the load-carrying capacity is defined as the maximum load before reaching a displacement $\delta = 15$ mm parallel to the load direction.

The experimental campaign conducted comprehended 15 specimens of single-doweled joints that connect three timber members made of glulam Scots pine (*Pinus sylvestris*) from GL24h strength as per EN 14080 [59]. Glulam members were chosen to avoid inherent defects of timber such as knots, which are distributed throughout the manufacturing process. The geometry of the specimens and the disposition of the wooden lamellas in the specimens are shown in Fig. 3, where the height of the middle member (H) is 320 mm and the heights of the side members (B) are 260 mm, the dowel diameter (d) is 12 mm, and the end-distance (a_3) is 90 mm ($7.5d$). The end-distance provided is slightly higher than the value suggested by EC5 [47], the objective was to prevent splitting of the wood members (see [60]). The friction between wood elements was not prevented in the experiments to replicate usual dowel-type joint conditions. Nonetheless, it is important to highlight that the design models presented in Section 3.1 do not consider friction effect, which may lead to a conservative design. Friction effects are usually not considered in the design models to account for uncertainties related to the connection assembly and behavior. Execution tolerances and shrink-swelling impact, for example, may result in poor contact between timber surfaces, which can compromise the mobilization of friction forces.

The deformation scheme resulted in failure mode II, therefore the inference models obtained from the experimental data are referred to this failure mode. The load–displacement curves are presented in Fig. 4. Fig. 5 shows the wood members and dowel after one of the tests, where there is no evidence of brittle failure. Here, it is important to highlight that the test stopped for a displacement of 15 mm to enable the assessment of the effective bending moment, $M_{y,eff}$. Elbashir, Branco, and Rodrigues [61] present monotonic tests of the same wood and similar dimensions where it can be observed that the load drop due to splitting failure occurs after 20 mm of displacement. That happened because the distance to the edge decreases, and splitting failure occurs in the side elements. Nonetheless, at this point, the embedment of the wood and the deformation of the dowel already reached excessive

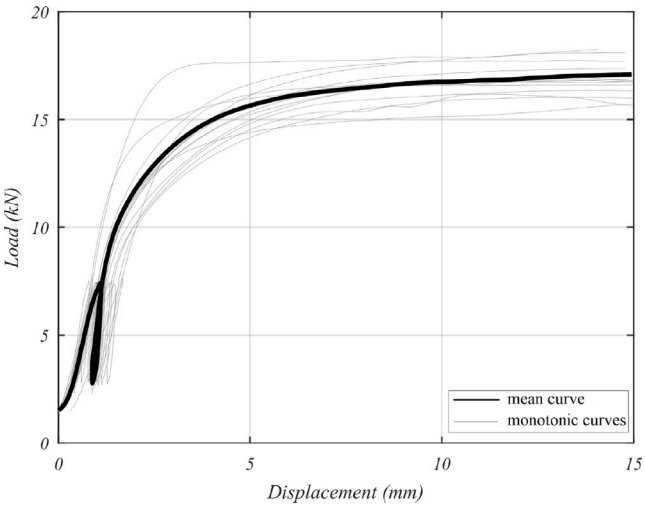

Fig. 4. Load–displacement curves for the monotonic experiments.

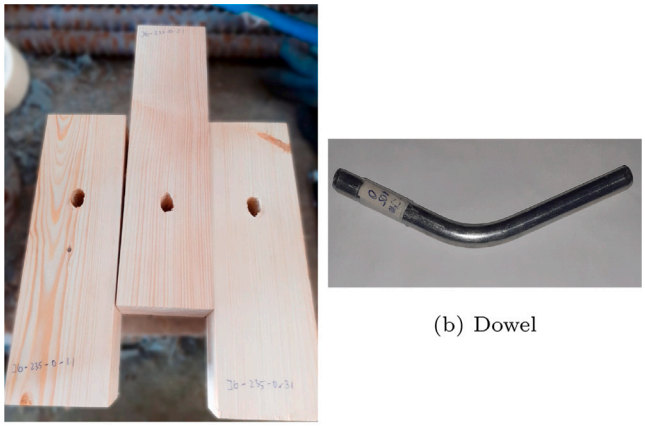

Fig. 5. Connection elements after the test.

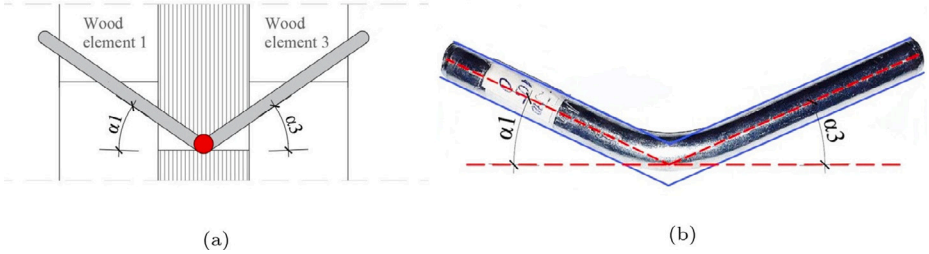

Fig. 6. Measurement representation of the bending angle: (a) deformation scheme, and (b) dowel after experiment.

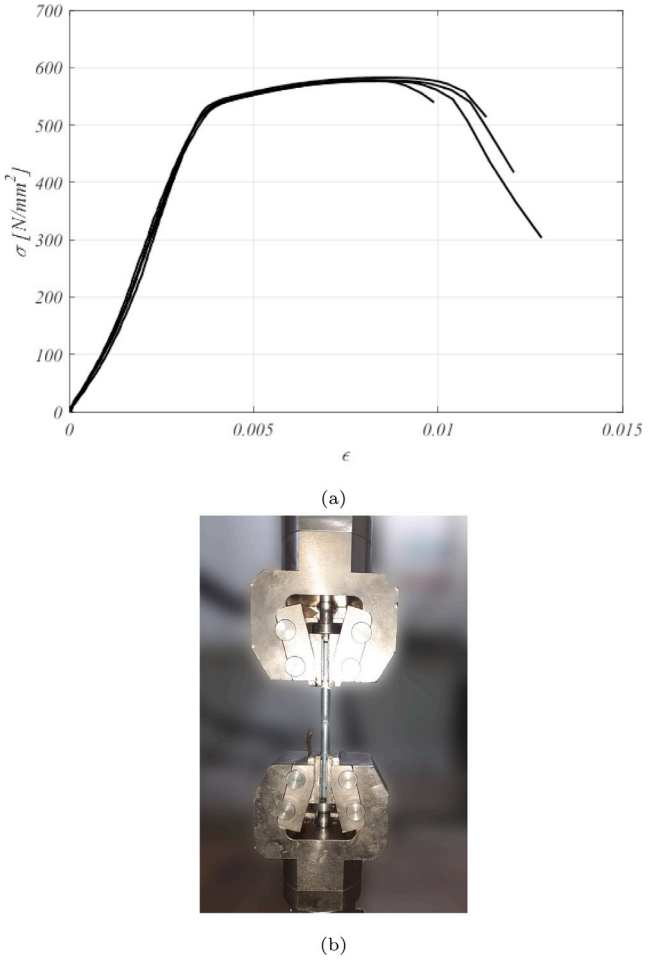

Fig. 7. Experimental tensile results: (a) stress–strain curve, and (b) dowel's rupture.

values in terms of structural behavior and the connection should be repaired.

Apart from load-carrying capacity R, the experimental tests allow to assess the impact of other parameters, such as the timber embedment strength (f_h) and the dowel's bending moment ($M_{y,eff}$). These parameters can be determined indirectly through empirical expressions and considering the measurements of the density (ρ) of each element, and the dowels' bending angle (α) (see Sections 2.1 and 2.2).

The steel dowels, as elastic–plastic members, present plastic deformation after reaching the yield moment. At this point, the load removal (unloading) enhances the so-called elastic recovery. Despite being considered here as the bending angle, α was measured at the end of the experiments, resulting from residual deformations of the dowels. Since there are no measures of the dowels' position during the test with respect to the wood elements, it was assumed that larger bending angles occurred when connected to smaller densities members. This assumption is made because the dowel's material has less variability than the wood material [7], and the wood embedment strength decreases with lower density values. This assumption is confirmed by the theoretical approach to determine α, given in Section 2.2. Fig. 6 illustrates how the measurements of α were obtained experimentally, where α_1 is related to the wood element 1 and α_3 to the wood element 3.

The results obtained for ρ and α are summarized in Table 1. The wood density (ρ) was measured for each element of each joint, hence the data of ρ_1, ρ_2, and ρ_3 are combined, constituting a 45 sample size. This sample is used to infer the statistical properties of ρ. In the case of α, its measurements are related to the side members merged with the middle member, there is a value for α between members 1 and 2, and another value between members 3 and 2 (see Fig. 6 for reference). Here, instead of 45 samples, there are 30 samples of α to conduct the statistical inference.

3.2. Tensile test

In order to characterize the steel used to manufacture the dowels, tensile tests were carried out according to the standard EN 10002-1 [62]. These tests were performed using a servo-controlled electromechanical universal testing machine, from Microtest, equipped with a 200 kN load cell. A clip-gauge was placed at the center of the specimen, so that the modulus of elasticity, E, and the proof strength $R_{p0.2}$, stress at which total extension is equal to 0.2% of the extensometer gauge length, could be determined. The clip-gauge was removed before the failure of the fastener to prevent its damage. Stress–strain curves of the four specimens (obtained with the clip-gauge) are presented in Fig. 7. As expected, the variation between tests is quite low. For that reason, only four specimens were tested. The tensile tests allow to conclude that the dowels have an average maximum strength R_m equal to 578.8 MPa, with a Coefficient of Variation (CoV) of 0.45%, while the average proof strength $R_{p0.2}$ is equal to 534.3 MPa with a CoV equal to 0.63%. These values allow concluding that the strength class S235 (f_u = 360 MPa) is over-passed by far, which can lead to an underestimation of the load-bearing capacity and misestimation of the failure mode of the connections under analysis. On the other hand, the average value of the modulus of elasticity (E) is equal to 181 GPa (CoV equal to 4.1%), which is below 210 GPa given by the standard EN 10025-2 [63]. The modulus of elasticity was retrieved through a linear regression analysis that disregarded the initial slip observed in the load–displacement curve presented in Fig. 7.

4. Statistical data modeling

4.1. Marginal inference

Mathematical modeling or representation of a random variable is a primary task in any probabilistic formulation, and needs to be

Table 1
Experimental results.

Variable	Mean value	Standard deviation	COV
ρ	463.31	46.33	10%
α	11.30	2.91	26%

conducted systematically. The first step is to collect data available, this will constitute the sample space for the respective random variable. In the case of material properties, for example, the data is obtained from experimental campaigns.

In general, there are two main stpdf required to the inference of the underlying distribution that better fits the available data: fitting some plausible models by parameter estimation and then selecting the one that presents the most appropriate fitting [64].

In this study, the available experimental data is fitted by a set of distributions (normal, lognormal, and extreme value type I) employing the maximum likelihood method, which consists in seeking the parameters that maximize the joint probability value of the random variable observations, that is, the likelihood function [65]. Once the parameters of the distributions have been determined, the probability distribution that best describes the data is selected. Various selection criteria exist to this end, e.g. the Akaike Information Criterion AIC [66], and the Kolmogorov–Smirnov KS hypothesis test [67]. Here, the inference of marginal distributions is performed through the UQLab [68] tool, where both AIC and KS tests are checked in order to determine the statistical model that best describe the data. In case of disagreement between criteria, a discussion shall be conducted to determine which criteria to follow.

4.2. Dependence modeling through the copula theory

When it comes to the reliability assessment of structures, the problem usually involves more than one random variable. Then, the uncertainty quantification requires not only the inference of the marginals, but also of the joint behavior. It has been suggested that the representation of the dependence behavior of the input random variables can play a significant role in the accuracy of reliability results [19]. With respect to the dependence structure, copula functions allow modeling the non-linear correlated behavior, which cannot be achieve through traditional approaches (e.g. the Nataf transformation [22]).

Copulas are defined as functions that join or "couple" multivariate distribution functions to their one dimensional marginal distribution functions. An M-copula is defined as an M-variate joint cumulative distribution function, CDF, $C : [0,1] \rightarrow [0,1]$ with standard uniform marginals [69]:

$$C(1,\dots,u_i,1,\dots,1) = u_i \forall u_i \in [0,1], \forall i = 1,\dots,M \tag{13}$$

Sklar's theorem allows to express joint CDFs in terms of their marginal distribution and a copula that represents the multivariate dependence structure. Considering a random vector $\boldsymbol{X} = (X_1, X_2, \dots, X_M)$, the theorem presented by Sklar [70] states that for its M-variate CDF, referred as $F_{\boldsymbol{X}}$, with marginals CDFs, referred as $F_1,\dots,F_M$, an M-copula $C_{\boldsymbol{X}}$ exists, such that for all $\boldsymbol{x} \in \mathbb{R}^M$ [71]:

$$F_{\mathbf{X}}(\mathbf{x}) = C_{\mathbf{X}}(F_1(x_1),\dots,F_M(x_M)) \tag{14}$$

Given $U_i = F_i(x_i), i = 1,\dots,M$, the copula from (14) is unique and has the expression:

$$C_{\mathbf{X}}(\mathbf{U}) = F_{\mathbf{X}}(F_1^{-1}(U_1),\dots,F_M^{-1}(U_M)), \mathbf{u} \in [0,1]^M \tag{15}$$

where the $F_i^{-1}(U_i)$'s are the inverse CDF's of the marginals.

Thus, the construction of the joint distribution consists of two separate problems. First, it is required to model the marginals F_i by the means presented in the previous section. Then, it is necessary to transform the original components of X_i into uniform random variables $u_i = F_i(X_i)$, that is:

$$\mathcal{T}^{(U)} : \mathbf{X} \rightarrow \mathbf{U} = (F_1(X_1),\dots,F_M(X_M))^T, \tag{16}$$

the joint CDF of $\mathbf{U} = (U_1,\dots,U_M)^T$ is the associated copula.

Given the joint probability density function, PDF, $f_{\mathbf{X}}(x) = dF_{\mathbf{X}}(x)/dx$, $f_{\mathbf{X}}$ can be derived using the chain rule. This procedure results in Eq. (17) in the case of multiple variables.

$$f_{\mathbf{X}}(x_1,\dots,x_M) = c_{1\dots M}\{F_1(x_1),\dots,F_M(x_M)\}\prod_{i=1}^{M} f_i(x_i) \tag{17}$$

where $c_{1\dots M}(\cdot)$ is an M-variate copula density function, defined by:

$$c(u_1,\dots,u_M) = \frac{\partial^M C}{\partial u_1 \cdots \partial u_M}(u_1,\dots,u_M) \tag{18}$$

To fully determine the joint distribution behavior, a copula family needs to be assigned to the data available. The inference of the copula function is analogous to the inference of marginals presented in the previous section. In this study, the copula inference process is done using the open source package Vine Copula Matlab [72].

Since copula functions are evaluated in the uniform space, the first step is to transform the data sample. For any random variable X_i in random vector $\mathbf{X}$, an uniform sample U_i can be obtained evaluating its marginal cumulative distribution function, that is, $u_i = F_i(x_i)$. A scheme of the idea is presented in Fig. 8.

If the problem involves the investigation behavior of only two random variables, the inference is conducted directly on the uniform pair sample. Which consists on estimating the copula parameters based on the maximum likelihood method (ML), and then selecting the optimum copula function for the variables through the Akaike information criterion (AIC). When the problem involves more than two random variables, a decomposition procedure is required (see [20]). In the scope of this paper, the statistical dependence investigation is referred to only two random variables.

5. Structural reliability analysis

5.1. General concepts

The main objective of a structural design is to fulfill the requirements for which it is being designed, in such a way that the capacity of the system must exceed the demand. There are always uncertainties involved in structural design. Thus, unfavorable combinations of the random variables involved may lead the structure to reach ultimate and/or service limit states. This event can be described by using limit state functions, given as follows:

$$g(\mathbf{X}) = R(\mathbf{X}) - S(\mathbf{X}) \tag{19}$$

where $\boldsymbol{X}$ is the vector of random variables; R($\boldsymbol{X}$) is the random variable related to resistance; and S($\boldsymbol{X}$) the random variable related to demand, usually seen as a load effect.

Failure occurs when $g(\boldsymbol{X}) \leq 0$. The probability of failure, P_f, is obtained by integrating the joint probability density function of the random variables, $f_{\boldsymbol{X}}(\mathbf{x})$, over the failure domain, where the demand exceeds the resistance [64].

$$P_f = P[g(\boldsymbol{X}) \leq 0] = \int_{g(\boldsymbol{X})\leq 0} f_{\boldsymbol{X}}(\mathbf{x})dx \tag{20}$$

Due to the difficulties to obtain analytical solutions for this integral, estimates for the failure probability are usually obtained via methods such as Monte Carlo Simulation.

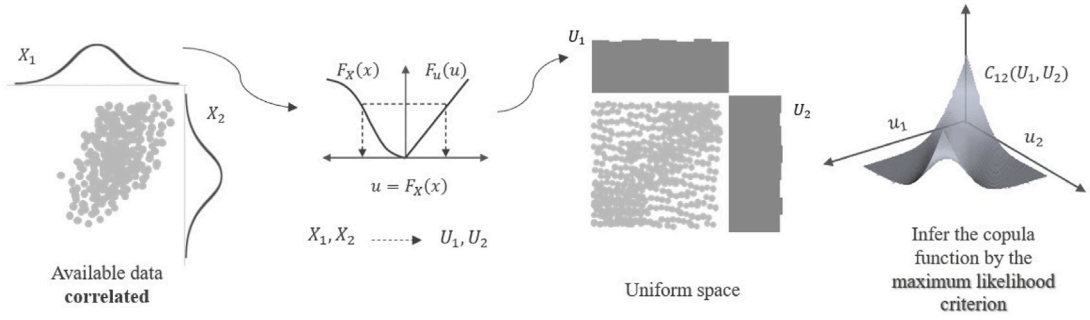

Fig. 8. Scheme for the copula inference.

5.2. Structural reliability methods: Monte Carlo simulation

The Monte Carlo simulation method applied to structural reliability consists of simulating the structural response for several random configurations of demand and resistance, based on their respective probability distributions. After the simulations, a statistical analysis is performed to determine the probability of failure [73,74]. Solution of reliability problems is obtained using an indicator function ($I[\mathbf{x}]$), where $I[\mathbf{x}] = 1$ if $g(\mathbf{X}) \leq 0$, and $I[\mathbf{x}] = 0$ if $g(\mathbf{X}) > 0$. Ultimately, an approximation of the probability of failure ($\hat{P}_f$) is given by the ratio between the number of failures (n_f) and the number of simulations (n_{si}) (see Eq. (21)). In the case of multiple failure modes, failure of the system can be defined by unions and/or intersections of single failure events.

$$\hat{P}_f = \frac{1}{n_{si}} \sum_{i=1}^{n_{si}} I[\mathbf{x}_i] = \frac{n_f}{n_{si}} \tag{21}$$

This method is often taken as a reference in reliability analyses, since $\hat{P}_f$ tends to the exact value of P_f when n_{si} tends to infinity. However, it should be emphasized that the smaller the probability of failure is, the bigger the number of simulations required, which can result in high computational demand. Besides this disadvantage, simulations by the Monte Carlo method are a robust and easy way to evaluate probabilistic problems.

In order to accelerate the convergence of the simulation, one can use a number of techniques presented in the literature, such as the so-called importance sampling. In this case, there is an attempt to generate samples closer to the limit state boundary, which accelerates convergence. Adopting an importance sampling distribution $h_{\mathbf{X}}(\mathbf{x})$, P_f can be estimated as in Eq. (22), where the ratio $\frac{f_{\mathbf{X}}(\mathbf{x}_i)}{h_{\mathbf{X}}(\mathbf{x}_i)}$ is the weight, w_i, of each simulation [74].

$$\hat{P}_f = \frac{1}{n_{si}} \sum_{i=1}^{n_{si}} I[\mathbf{x}_i] \frac{f_{\mathbf{X}}(\mathbf{x}_i)}{h_{\mathbf{X}}(\mathbf{x}_i)} = \frac{1}{n_{si}} \sum_{i=1}^{n_{si}} I[\mathbf{x}_i] w_i \tag{22}$$

The importance sampling distribution may be obtained by centering the original distribution at the most probable failure point (MPP) over the failure surface, since this is the point that contributes the most to the P_f. The reliability problem can be transformed to the standard normal space, where all random variables are converted to equivalent variables with standard normal distribution. In this space, the MPP corresponds to the closest point between the origin and the failure surface $g(\mathbf{X}) = 0$, such distance is defined as the reliability index (β), which refers to the safety level of a structure. The present study employees the Finite-Step-Length algorithm (FSL) to search for the MPP [75], and uses Monte Carlo simulation with importance sampling based on the MPP to solve the structural reliability problems of interest. Local sensitivity indexes may obtained based on the MPP, within the normal standard space, by taking the unit vector α in the direction of $\nabla g(\mathbf{X})$, which is the gradient vector of the limit state function in the normal standard space. The components of α_i can be defined as follows:

$$\alpha_i = -\frac{\partial \beta}{\partial x_i^*} \tag{23}$$

As $\sum \alpha_i^2 = 1$, the components of α_i^2 indicates the relative contribution of the random variable $\mathbf{X}_i$ in the composition of the probability of failure, directly related to the first order reliability method (FORM) [64,74].

5.3. Sampling method

The simulation process related to Monte Carlo methods depends fundamentally on the generation of random numbers according to the available statistical information on the random variables involved. Traditional methods usually resort to implemented pseudo-random number generating systems that computationally produce uniformly distributed values [64]. These random values are taken to their respective marginal distributions through the inverse function of their cumulative probability distribution. When there is correlation among the variables, it can be introduced in the form of linear pairwise correlation coefficients through the Nataf transformation.

Theses approaches are implemented because there usually is a lack of information regarding the joint behavior of the random variables. Alternatively, since the Copula theory allows the construction of the joint distribution, a sampling method based on it is desirable. The sampling process for two random variables is presented next. For a problem involving multidimensional correlation see [20].

1. Obtain the joint PDF via copula functions, this is summarized in Section 4.2;
2. Generate a sample (r_1, r_2) from a multidimensional independent uniform distribution, where n is the number of random variables of the problem;
3. Take the uniform sample to its joint distribution:

$$f(x_1, x_2) = f_1(x_1) \cdot f_2(x_2) \cdot c_{12}(F_1(x_1), F_2(x_2))$$

   (a) let $u_1 = r_1$, and then obtain $x_1 = F_1^{-1}(u_1)$ (this step consists of transforming the uniform variable to its marginal distribution);
   (b) let

$$r_2 = h_{21}(u_2, u_1) = F_{2|1}(x_2|x_1) = \frac{\partial C_{12}(F_1(x_1), F_2(x_2))}{\partial F_1(x_1)}, \tag{24}$$

   reorganizing leads to $u_2 = h_{21}^{-1}(r_2, u_1)$ (this step introduces correlation between variables u_1 and u_2), and then $x_2 = F_2^{-1}(u_2)$ (x_2 is obtained transforming the uniform variable to its marginal distribution);

4. A sample for the random vector $\mathbf{X}$ is obtained.

6. Statistical dependence investigation

6.1. A theoretical view of the proposed investigation

In order to discuss the idea behind the reliability investigation from a theoretical point of view, it is assumed that there is a random variable X_1, whose probability distribution is known, and there are two other random variables X_2 and X_3, which depend on X_1. That is:

$$X_2 = f(X_1) \tag{25}$$

$$X_3 = h(X_1) \tag{26}$$

It is also assumed that there is a limit state function $g(X_2, X_3)$ that depends both on X_2 and X_3. For example:

$$g(X_2, X_3) = X_2 - X_3 \tag{27}$$

Solution of this problem can be addressed through different approaches. It is possible to obtain samples of X_2 and X_3, and infer their probability distribution behavior by means of statistical data modeling. In this case, the source of uncertainties, given by X_1, is forgotten, and the problem is solved based on the secondary variables. For this approach, the probability of failure $P_f[g(X_2, X_3) \leq 0]$ could be calculated disregarding possible correlations. On the other hand, correlation coefficients could be inferred from the samples of X_2 and X_3, and P_f could be recalculated considering a linear correlation. Finally, a copula function could be fitted to the joint sample $[X_2, X_3]$, and the problem could be solved again considering a linear/non-linear correlation.

Alternatively, the problem can be looked at from the point of view of the correlation origin. This approach consists of solving the original problem, given by $g(X_1)$. For the example given in Eq. (27), that would mean solving the limit state function in the format of (28).

$$g(X_1) = f(X_1) - h(X_1) \tag{28}$$

The methodology described herein aims to investigate how much the solution where the correlation is modeled via copula functions differs from common reliability approaches (linear correlation or consideration of independence between random variables), for the problems at hand. Moreover, it is intended to verify if the copula approach can recover the solution of the original problem, aiming to briefly investigate, in terms of the problem of interest, under what circumstances the copulas are flexible enough to do this. Note that the copula approach becomes unnecessary if it is possible to solve the problem using the common source of uncertainties, although many times in practice the underlying random variables are not known.

6.2. Application to dowel-type timber joints

The idea presented above is developed in the context of dowel-type timber joints, where the secondary variables X_2 and X_3 are $M_{y,eff}$ and f_h, and their source of dependency X_1 is ρ. The investigation is mainly focused on the analysis of the failure modes where failure is characterized by the plastic bent of the dowel. This is justified because the bending capacity does not affect the load-carrying capacity of connections with rigid fasteners (failure modes characterized by the embedment of the wood) [35] or brittle failure modes (e.g. splitting or plug shear), and therefore, in this situation the correlation modeling between $M_{y,eff}$ and f_h should not present high impact on the probability of failure of the connection.

6.3. Investigation procedure

The investigation is conducted on the reliability of the design of a dowel-type timber joint, where the related limit states are referred to the failure modes presented in Fig. 1. The interaction model between failure modes adopted is the one proposed by Köhler [7], where failure modes I and Ia are considered brittle and models II and III are ductile.

System failure events are given by combinations of individual failure modes. In this case, symmetry of the connection must be disregarded so that the possible combinations are correctly identified. The system fails when one of the side members fails under mode I, when the middle member fails under mode Ia, or when the side members achieve failure modes II or III. A set of limit states associated in series are defined to assess the system reliability of the single fastener connection:

$$g_1 = 2z_d R_{I,1} X_I - S_G - S_Q \tag{29a}$$

$$g_2 = 2z_d R_{Ia,2} X_I - S_G - S_Q \tag{29b}$$

$$g_3 = 2z_d R_{I,3} X_I - S_G - S_Q \tag{29c}$$

$$g_4 = z_d(R_{II,1} + R_{II,3})X_{II} - S_G - S_Q \tag{29d}$$

$$g_5 = z_d(R_{III,1} + R_{III,3})X_{III} - S_G - S_Q \tag{29e}$$

$$g_6 = z_d(R_{II,1} X_{II} + R_{III,3} X_{III}) - S_G - S_Q \tag{29f}$$

$$g_7 = z_d(R_{III,1} X_{III} + R_{II,3} X_{II}) - S_G - S_Q \tag{29g}$$

where z_d is a design variable related to the resistance of the joint; S_G is the permanent load; S_Q is the variable load; and X_I, X_{Ia}, X_{II} and X_{III} are the model uncertainties related to each failure mode, which try to cover deviations and simplifications related to the probabilistic modeling and the limit state equations. The design variable z_d is derived in accordance with Eurocode 5 [47], as given in Eq. (30).

$$z_d = \frac{\gamma_G S_{G,k} + \gamma_Q S_{Q,k}}{2R_k} \gamma_M \tag{30}$$

where $S_{G,k}$ and $S_{Q,k}$ are the characteristic loads; γ_M, γ_G and γ_Q are the partial safety factors referred to strength, permanent, and variable loads, respectively; R_k is the characteristic value for resistance, given as the minimum value of Eqs. (1) using the characteristic values for the embedment strength and the fastener bending moment. In Eq. (30), R_k is doubled because its value is referred per connection shear plane.

For the reliability assessment, first $M_{y,eff}$ and f_h are taken as random variables. Based on the experimental measurements of ρ (see 3.1), a sample of f_h is obtained by means of the Eurocode 5 [47] expression, given in (2). Likewise, a sample of $M_{y,eff}$ is obtained based on the experimental measurements of α and ρ according to Eq. (5). A statistical inference is performed on the samples obtained of $M_{y,eff}$ and f_h, both in terms of their marginal and joint behavior. This process is equivalent to the idea presented in Eq. (27). A scheme is illustrated in Fig. 9.

When the problem is addressed from the correlation origin viewpoint, the random variables concerning the connection strength are ρ and f_u. Here, f_h and $M_{y,eff}$ are functions of ρ, and they are directly determined from Eqs. (2) and (5), respectively, during the reliability analysis. However, α is now assessed through the theoretical approach presented in Eqs. (6), (7), (8), and (9). Evaluating the correlation from the origin, the results taken as references are obtained. This approach is equivalent to the idea presented in Eq. (28). Fig. 10 presents a scheme of the inference process for the correlation origin.

7. Statistical inference of the random variables

7.1. Marginal information of the random variables

Table 2 summarizes the statistical information of the inferred variables, and of the other input variables involved in the problem. With respect to the last group, the permanent load, S_G, and the variable load, S_Q, are based on Köhler [7]. The mean value of f_u is considered to be the one obtained in the tensile tests, but the distribution and coefficient of variation are based on Köhler [7].

Additionally to the variables presented, the model uncertainty is introduced. Köhler [7] indicates values for model uncertainties with

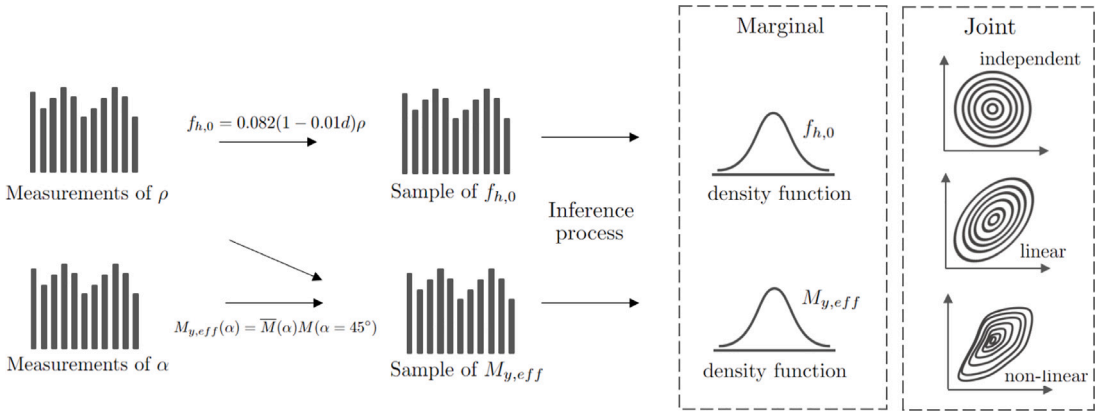

Fig. 9. Scheme for the inference process of the data.

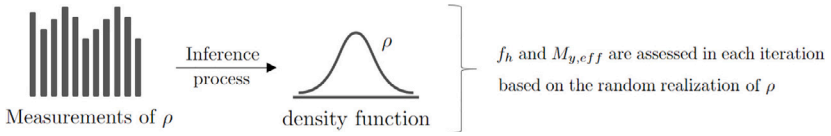

Fig. 10. Scheme for the inference process of the correlation origin.

Table 2
Statistical information of the input variables.

	Timber density ρ	Tensile strength f_u [MPa]	Embedment strength f_h [MPa]	Effective bending moment M_y [N mm]	Permanent load S_G [N]	Variable load S_Q [N]
Distribution	Lognormal	Lognormal	Lognormal	Normal	Normal	Gumbel
Mean value	463.31	578.80	33.43	102 770	1000	1200
st. dev.	46.33	23.15	3.34	51 384	100	480
CV	0.10	0.04	0.10	0.05	0.10	0.40
Fractile	5%	5%	5%	5%	50%	98%
char. value	391.25	534.30	28.23	94 315	1000	2444
par. safety fac.			$\gamma_M = 1.3$		$\gamma_G = 1.35$	$\gamma_Q = 1.5$

Table 3
Model uncertainties for the different failure modes.

	Mean	st. dev.	CV	Distribution
X_I, X_{Ia}	0.8	0.12	0.15	Lognormal
$X_I I$	1.2	0.15	0.12	Lognormal
$X_I I I$	1.3	0.20	0.15	Lognormal

respect to each failure mode of single dowel-type joints in double shear, given in Table 3.

As for the geometry parameters, the members thickness are equal for the three members $t_1 = t_2 = t_3 = 60$ mm; the dowel's diameter is $d = 12$ mm; and the fastener placing is $a_3 = 7.5d$ (see Fig. 3).

7.2. Correlation of the random variables

A first step to investigate the correlation hypothesis between f_h and $M_{y,eff}$ is to analyze their scatter plot, shown in Fig. 11 together with the copula function that best fits the data. The data analyzed is referred to the experimental results obtained for failure mode II, and are analyzed separately for the side and middle members. If the scatter plot shows a particular pattern, it is probable that the data is correlated.

For the side members, it was found that $M_{y,eff}$ tends to decrease with the increase of $f_{h,s}$, therefore, the variables are negatively correlated. To understand this behavior, one can picture the deformation scheme of the connection in this failure mode: when $f_{h,s}$ present small values the dowel bends easily, larger deformations can lead to a full plastic hinge in the dowel (positioned in the middle member), where $M_{y,eff}$ reaches its maximum capacity; on the other hand, for high values of $f_{h,s}$, less bending occurs in the dowel, therefore, the plastic hinge partially forms and, consequently, $M_{y,eff}$ is partially mobilized. This behavior can be noted also in terms of the stiffness of the connection. If the embedment strength increases, it is expected that the dowel strength will contribute more to the load-carrying capacity of the connection, and, therefore, the stiffness would be higher. The correlation between the embedment strength and the slip modulus of the experiments was calculated via the Pearson correlation coefficient and a positive value (0.12 and 0.14 for the right and left member, respectively) was found. Although the correlation is small, this indicates that variations of the embedment strength represent some variation on the stiffness of the connection. For the middle members, the correlation behavior found is reversed, that is, $M_{y,eff}$ tends to increase with the increase of $f_{h,m}$. The explanation for this lies in the presence of the plastic hinge in the dowel positioned in the middle member. Once again visualizing the deformation scheme: with the increase in $f_{h,m}$, the resistance against the dowel's bending increases, and hence, it forms a plastic hinge, leading $M_{y,eff}$ to reach its maximum capacity. No correlation was found between the slip modulus and the embedment strength of the middle element.

The copula approach is used to quantify this correlated behavior. The dependence structure that best describes the data is inferred, resulting in the Frank copula with parameter $\theta = -2.7201$ for the side members. The Frank copula is a symmetric Archimedean copula with a positive slope and the absence of a tail on either end of the scatter plot. The correlation is represented via an uniform cloud along the full correlation path. For the middle members, the inference resulted in the Gaussian copula with parameter $\theta = 0.1913$. For the Gaussian copula is a copula from the Clayton family where the parameter θ corresponds

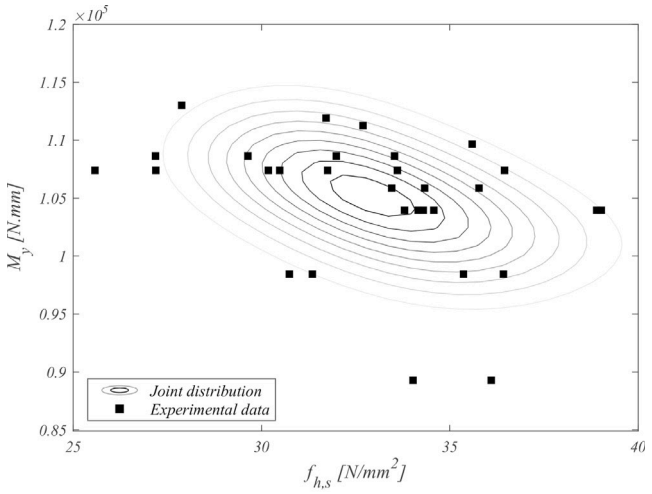

(a) Side member

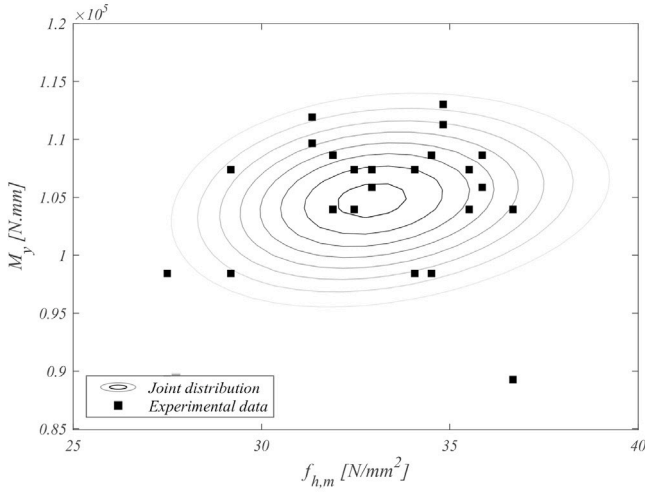

(b) Middle member

Fig. 11. Joint distribution behavior for failure mode II.

to the Pearson's correlation coefficient. The Gaussian copula has more probability concentrated in the tails than does the Frank copula.

In order to compare the copula representation with linear pairwise correlation coefficients, the Gaussian copula is also fitted to the side members data resulting in $\theta = -0.3780$. The Gaussian copula is equivalent to the more traditional approach of considering linear correlations via the Nataf transformation [23]. Comparing the Gaussian copula results with other copulas which better fit the data, the impact of the correlation modeling can be inferred. For the middle member, the data already presents linear correlation, thus there is no difference to be investigated.

8. Results and discussion

8.1. Comparison between correlation models

The investigation regarding the influence of correlation modeling in the reliability results starts with the analysis of failure mode II, apart from the system, for $t = 60$ mm. Such decision is made because the dependence structure was inferred from the experimental data and all the 15 specimens tested, with dimensions $t_1 = t_2 = t_3 = 60$ mm, resulted in failure mode II.

Table 4
Reliability results for failure mode II.

	Independent	Gaussian	Frank	Reference
β	5.0932	5.0867	5.0820	5.0902
P_f	1.7602E−7	1.8219E−7	1.8673E−7	1.7883E−7
CV_{P_f}	0.01	0.01	0.01	0.01

Table 5
Reliability results for failure mode II without S_Q and X_{II}.

	Independent	Gaussian	Frank	Reference
β	3.5371	3.6138	3.6176	3.5937
P_f	2.0227E−4	1.5087E−4	1.4867E−4	1.6301E−4
CV_{P_f}	0.01	0.01	0.01	0.01

Results are obtained via Importance Sampling Monte Carlo method, with a total of 1E5 simulations. A coefficient of variation of the probability of failure (CV_{P_f}) of 0.01 or less is achieved. The results are given in Table 4, and are referred according to the side members dependence structures discussed in Section 7.2. That is, the reliability index is determined considering independence between f_h and $M_{y,eff}$, Gaussian copula (linear correlation), and the Frank Copula (resulted from the inference process). The reference value presented is the reliability index computed from the correlation origin viewpoint, where the correlation is implicitly considered by means of the variables dependence to the wood density ρ. By taking the reliability index of this approach as a reference, it was possible to infer the impact of the correlation modeling via distinct methods.

The influence of the correlation approach on the failure probability was found to be very small in this case. For a better understanding of the problem, sensitivity indexes based on the MPP are also computed herein. It is noted that the parameter with greater influence on the probability of failure is S_Q (variable load). The large influence of S_Q is directly related to its large variability. Distinct studies consider different coefficient of variations for S_Q ranging from 0.20 to 0.60 (e.g. [74,76,77]) for S_Q. Considering 0.20 instead of 0.40, for example, leads to a smaller, but still high, sensitivity index of 0.75 for S_Q, while the sensitivities with respect to f_h and $M_{y,eff}$ (important variables from the copula point of view) are slightly increased to 0.03 and 0.02, respectively.

Another variable with large impact on the P_f is the model uncertainty, as already reported in the literature [7]. In an attempt to focus on the influence of the copula functions, both the model uncertainty and the variable load are taken out of the analysis. To keep the order of magnitude of the P_f, the permanent load is increased by 1 kN. Even in this situation, the results for the different correlation models remain close, as shown in Table 5. However, it is seen that results obtained using the Gaussian and Frank copulas are slightly closer to the reference values.

The reliability analysis conducted herein for the dowel-type timber joints indicates that, unless significantly nonlinear correlations exist among the data, the results obtained by applying the different copulas will probably be very close. However, it is difficult to establish beforehand if the correlation is nonlinear enough, since the reliability indexes are also very dependent on the limit state functions and on the other variables. Nevertheless, the results shown herein indicate that for this particular case study a simpler approach, e.g. using the Nataf transformation, would be enough to deal with the correlation.

8.2. Influence of the tensile strength

As seen on Section 3.2, the experimental results on the ultimate tensile strength, f_u, proved to be significantly larger than the value pointed out by the company's catalog. The impact of this finding in the reliability index is investigated here. The reliability is computed

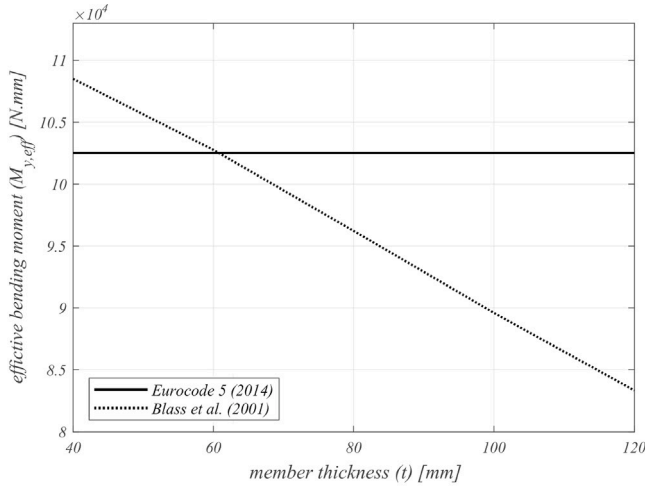

(a) Failure mode II

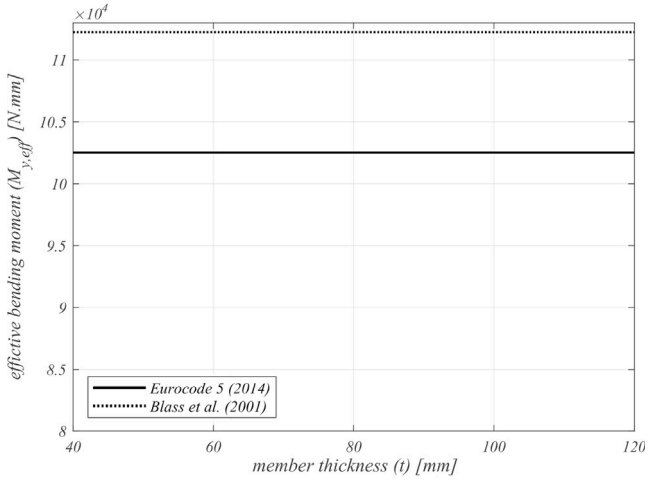

(b) Failure mode III

Fig. 12. Comparison of the Blass et al. [31] and Eurocode 5 [47] equations varying with the member thickness ($t_1 = t_2 = t_3 = t$).

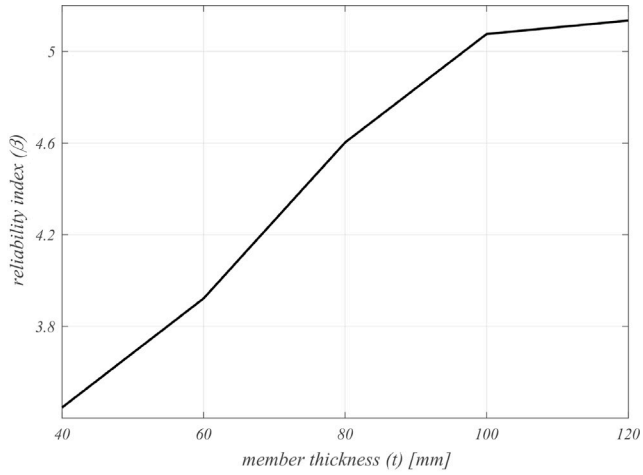

(a) System reliability

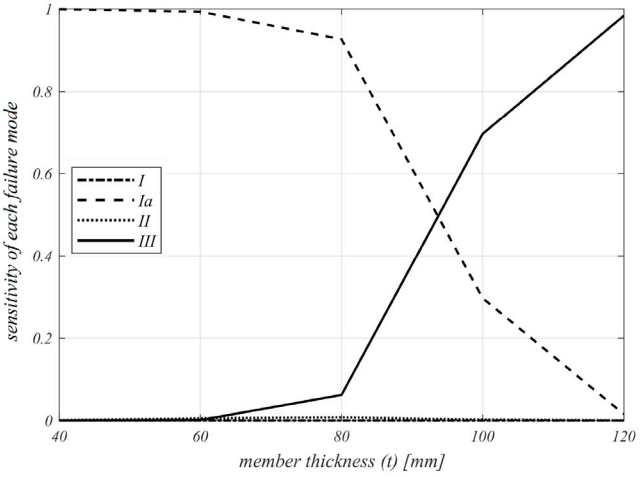

(b) Influence of each failure mode

Fig. 13. Results for the system reliability assessment for $t_1 = t_2 = t_3 = t$.

for the same situation of the previous subsection, but in this case the connection is design for a f_u = 360 MPa instead of the characteristic value of f_u = 534.30 MPa found on the experimental tests. The statistical information of the random variable remains the same, that is, it assumes the values presented in Table 2. By doing this, it is possible to verify how the reliability index behaves in a situation where the connection is designed according to the company's catalog, but the actual value is larger. A β = 5.34 was found, presenting an increase of 5% to the connection designed according to the experimental results (see Table 4). This indicates an overly conservative design scenario for the considered failure mode. Moreover, it represents a misestimation of the failure mode prone to occur, since the ductility of the connection is influenced by such property. For the present case, the failure mode predicted corresponds to mode III, but the resulting failure mode of the experiments was actually failure mode II (see Fig. 1 for reference).

8.3. Reliability assessment varying the member thickness

It was seen that the EC5 [47] equation to assess $M_{y,eff}$ is a simplification of the model presented by Blass et al. [31]. The latter was employed in this paper as it defines $M_{y,eff}$ as a function of f_h and α. In view of this, a comparison is conducted to address the main differences and possible disagreement between models.

The theoretical equation to assess α for failure mode II (Eq. (6)) depends on the member thickness. Therefore, the effective bending moment ($M_{y,eff}$) is indirectly influenced by this property. Such dependence is not considered in the normative expression. In Fig. 12(a), the Blass et al. [31] approach to assess $M_{y,eff}$ is compared with the Eurocode 5 [47] equation for different values of t, the wood density is fixated in the mean value obtained in the experiments. The results show that $M_{y,eff}$ significantly decreases with the increase of t, and that the normative equation overly estimates $M_{y,eff}$ for larger values of the member thickness.

The behavior of $M_{y,eff}$ for different member thicknesses is also assessed for failure mode III. In opposite to the results obtained in Figs. 12(a) and 12(b) shows that the normative equation underestimates $M_{y,eff}$ in comparison with Blass et al. [31]. Beyond that, in this situation $M_{y,eff}$ does not vary with t, which is in consistency with the normative equation.

The analysis that follows focus on a parametric investigation of the normative design model and extrapolates the experimental campaign conducted herein. Nonetheless, a sensitivity analysis of the failure modes with respect to the system failure is desirable to assess the impact of the design model in the probability of failure of the connection. By designing the connection following EC5 and performing system reliability analysis considering the correlation origin, the reference results

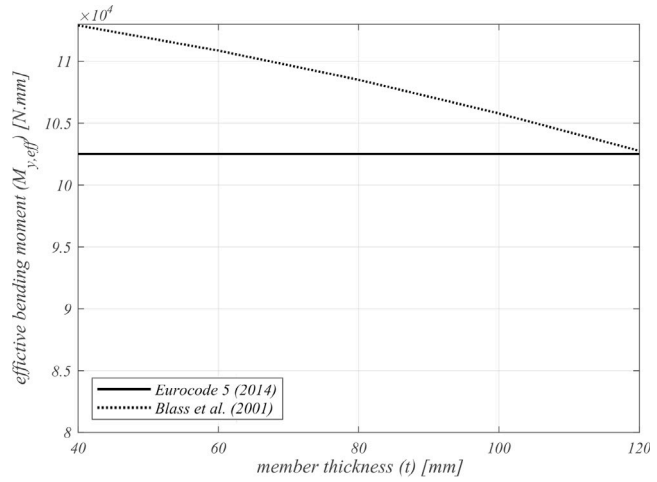

(a) Failure mode II

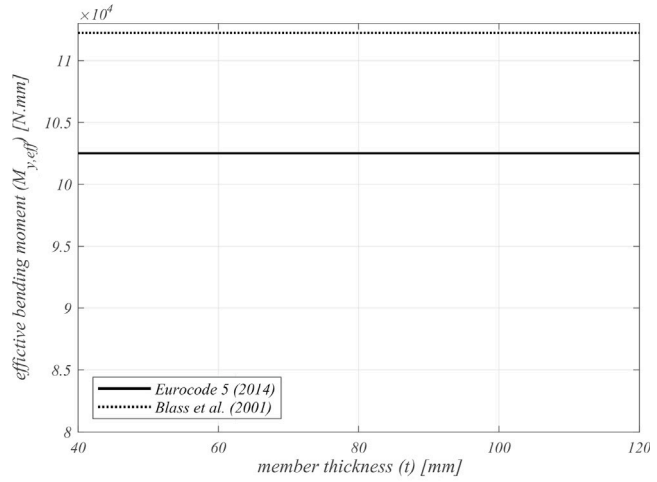

(b) Failure mode III

Fig. 14. Comparison of the Blass et al. [31] and Eurocode 5 [47] equations varying with the member thickness ($2t_1 = t_2 = 2t_3 = t$).

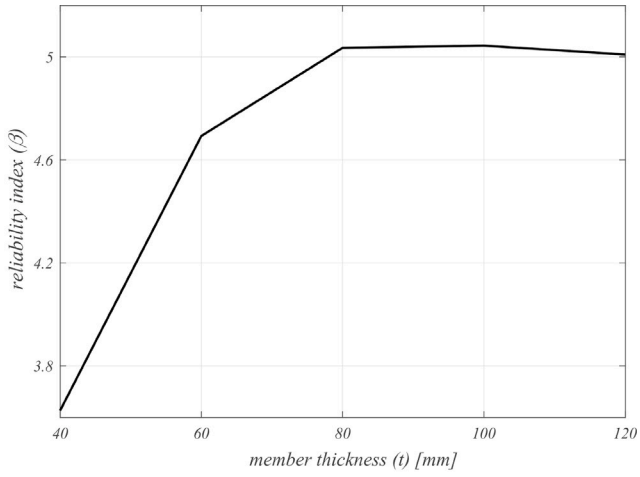

(a) System reliability

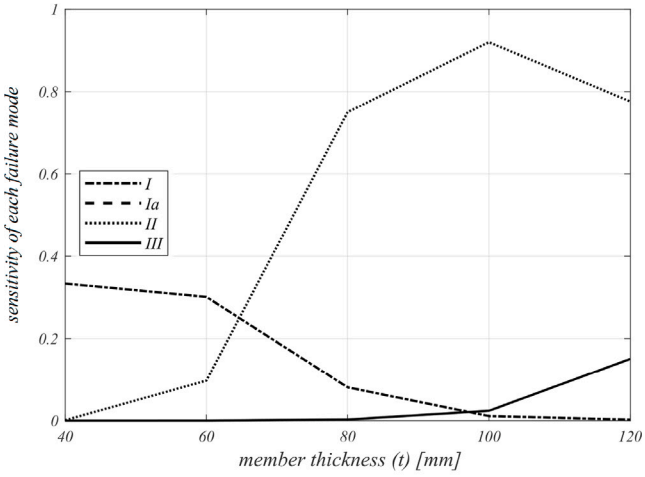

(b) Influence of each failure mode

Fig. 15. Results for the system reliability assessment for $2t_1 = t_2 = 2t_3 = t$.

illustrated in Fig. 13 are obtained. It is noteworthy that by applying the design variable z_d in the limit state equation, the relation between the connection strength and the loading applied is approximately constant for the different member thicknesses adopted.

It can be seen that β increases with the increase of the member thickness; this behavior can be related to the predominant failure mode. The dominant failure mode changes depending on the thicknesses involved. When failure mode III becomes predominant, the reliability index increases, which tends to occur for greater thicknesses (higher slenderness ratio). On the other hand, if failure mode Ia predominates, the reliability index presents smaller values. The main difference between these failure modes is the mobilization of the dowel's bending capacity. The resistance mechanism of failure mode Ia depends only on the wood embedment strength, which presents greater variability. Fig. 12 presents the difference between the model adopted in this paper (Blass et al. [31]) and EC5, when assessing the effective bending moment, $M_{y,eff}$. For failure mode II, for an increasing thickness, EC5 would overestimate $M_{y,eff}$. Nonetheless, since the diameter of the dowel remains fixed, larger thickness yields to higher slenderness and failure mode III is prone to occur. Therefore, the difference found in Fig. 12 does not present a concern with respect to the EC5 model.

The same investigation is conducted for $2t_1 = t_2 = 2t_3 = t$. This design strategy is often taken as an attempt to avoid brittle failure of the middle element. Analyzing the effective moment and the reliability of the system together (see Figs. 14 and 15, respectively), it is noted that the overall behavior of the system reliability remains. The governing failure mode is now related to failure mode II, but in this scenario the behavior of $M_{y,eff}$ for $2t_1 = t_2 = 2t_3 = t$ according to the approach proposed by Blass et al. [31] is closer to the result of the normative equation.

9. Conclusions

This study presented reliability analyses in the context of a single doweled timber-to-timber joint. Correlation between the timber embedment strength and the dowel bending moment capacity, which are parameters of significant impact on the design of dowel-type timber joints, were considered. Traditional distribution fitting as well as copula functions were implemented to describe the dependence between these parameters, using data from an experimental campaign.

The experimental campaign showed that the f_h, and the effective bending moment of the dowels, $M_{y,eff}$ are correlated, as expected. But via the reliability analyses, it was shown that this correlation does not

significantly impact the probability of failure of the connection. The results showed that the impact of correlation modeling on the results was small in this case, so that the copula functions could be replaced by simpler approaches. Beyond that, the experimental results on the ultimate tensile strength of the fasteners proved to be significantly larger than the value pointed out by the company's catalog. This overstrength represents an increase of 5% in the reliability index related to the design. However, it may lead to a misestimation of the failure mode prone to occur.

A sensitivity analysis led to the conclusion that small changes on the values of the resistance variables have little influence on the probability of failure. Therefore, improving their characterization represents a minor improvement in the reliability results. This is an important finding since it validates existing reliability models that do not consider correlation between the timber embedment strength, f_h, and the effective bending moment of the dowels, $M_{y,eff}$. Nonetheless, this conclusion may prove wrong regarding brittle failure modes, which were beyond the scope of this paper.

Although the impact of using copula in this study was small, the reliability investigation allowed to conclude that these functions are a viable tool to represent dependence structure between random variables. The results obtained using copula functions to represent the correlation were very close to those obtained considering the correlation from its origin. Therefore, in a situation where the correlated variables significantly influence the probability of failure and the correlation shows non-linearity, representing the correlation behavior through copulas may be an interesting approach to achieve reliable results.

CRediT authorship contribution statement

Caroline D. Aquino: Conceptualization, Methodology, Software, Validation, Investigation, Writing – original draft, Writing – review & editing. **Leonardo G. Rodrigues:** Conceptualization, Methodology, Investigation, Writing – original draft, Writing – review & editing. **Jorge M. Branco:** Conceptualization, Methodology, Writing – review & editing, Supervision. **Wellison J.S. Gomes:** Conceptualization, Methodology, Writing – review & editing, Supervision.

Declaration of competing interest

The authors declare that they have no known competing financial interests or personal relationships that could have appeared to influence the work reported in this paper.

Data availability

Data will be made available on request.

Acknowledgments

This work was financed by FEDER funds through the Competitivity and Internationalization Operational Programme COMPETE, Portugal 2020, and by national funds through FCT – Foundation for Science and Technology within the scope of the Timquake project POCI-01-0145-FEDER-032031. The authors also thank the Brazilian Research Council (CNPq) for sponsoring this research through the grant 302489/2017-7 and through the scholarship grant conceded to the first author.

References

[1] Frühwald E, Serrano E, Toratti T, Emilsson A, Thelandersson S. Design of safe timber structures - how can we learn from structural failures in concrete, steel and timber?. TVBK-3053, Division of Structural Engineering, Lund University; 2007.
[2] Köhler J. A probabilistic framework for the reliability assessment of connections with dowel type fasteners, in: Proceedings of the 38th CIB-W18 meeting; 2005.
[3] Foliente GC. Design of timber structures subjected to extreme loads. Prog Struct Eng Mater 1998;1(3):236–44. http://dx.doi.org/10.1002/pse.2260010304.
[4] Munch-Andersen J, Dietsch P. Robustness of large-span timber roof structures—two examples. Eng Struct 2011;33(11):3113–7. http://dx.doi.org/10.1016/j.engstruct.2011.03.015.
[5] Hansson E. Analysis of structural failures in timber structures: Typical causes for failure and failure modes. Eng Struct 2011;33(11):2978–82. http://dx.doi.org/10.1016/j.engstruct.2011.02.045.
[6] Faber MH, Köhler J, Sorensen JD. Probabilistic modeling of graded timber material properties. Struct Saf 2004;26(3):295–309. http://dx.doi.org/10.1016/j.strusafe.2003.08.002.
[7] Köhler J. Reliability of timber structures (Ph.D. thesis), Zurich, Swiss: Institute of Structural Engineering, Swiss Federal Institute of Technology; 2007.
[8] Jenkel C, Leichsenring F, Graf W, Kaliske M. Stochastic modelling of uncertainty in timber engineering. Eng Struct 2015;99:296–310. http://dx.doi.org/10.1016/j.engstruct.2015.04.049.
[9] Jockwer R, Fink G, Köhler J. Assessment of the failure behaviour and reliability of timber connections with multiple dowel-type fasteners. Eng Struct 2018;172:76–84. http://dx.doi.org/10.1016/j.engstruct.2018.05.081.
[10] Leijten A, Köhler J, Jorissen A. Review of probability data for timber connections with dowel-type fasteners, in: Proceedings of CIB-W18/paper; 2004, p. 37–7.
[11] Sandhaas C, Ravenshorst GJP, Blass HJ, Van de Kuilen JWG. Embedment tests parallel-to-grain and ductility aspects using various wood species. Eur J Wood Wood Prod 2013;71(5):599–608. http://dx.doi.org/10.1007/s00107-013-0718-z.
[12] Yurrita M, Cabrero JM. New criteria for the determination of the parallel-to-grain embedment strength of wood. Constr Build Mater 2018;173:238–50. http://dx.doi.org/10.1016/j.conbuildmat.2018.03.127.
[13] Kirkegaard PH, Sørensen JD, Čizmar D, Rajčić V. System reliability of timber structures with ductile behaviour. Eng Struct 2011;33(11):3093–8. http://dx.doi.org/10.1016/j.engstruct.2011.03.011.
[14] Rodrigues LG, Branco JM, Neves LA, Barbosa AR. Seismic assessment of a heavy-timber frame structure with ring-doweled moment-resisting connections. Bull Earthq Eng 2018;16(3):1341–71. http://dx.doi.org/10.1007/s10518-017-0247-y.
[15] Rosowsky DV. Evolution of probabilistic analysis of timber structures from second-moment reliability methods to fragility analysis. Struct Saf 2013;41:57–63. http://dx.doi.org/10.1016/j.strusafe.2012.10.004.
[16] Glynn PW, Iglehart DL. Importance sampling for stochastic simulations. Manage Sci 1989;35(11):1367–92. http://dx.doi.org/10.1287/mnsc.35.11.1367.
[17] Melchers RE. Search-based importance sampling. Struct Saf 1990;9(2):117–28. http://dx.doi.org/10.1016/0167-4730(90)90003-8.
[18] Zhang Y, Der Kiureghian A. Two improved algorithms for reliability analysis. In: Reliability and optimization of structural systems. Boston, MA: Springer; 1995, p. 297–304. http://dx.doi.org/10.1007/978-0-387-34866-7_32.
[19] Torre E, Marelli S, Embrechts P, Sudret B. A general framework for data-driven uncertainty quantification under complex input dependencies using vine copulas. Probab Eng Mech 2019;55:1–16. http://dx.doi.org/10.1016/j.probengmech.2018.08.001.
[20] Jiang C, Zhang W, Han X, Ni BY, Song LJ. A vine-copula-based reliability analysis method for structures with multidimensional correlation. J Mech Des 137(6):061405. http://dx.doi.org/10.1115/1.4030179.
[21] Wang F, Li H. System reliability under prescribed marginals and correlations: Are we correct about the effect of correlations? Reliab Eng Syst Saf 2018;173:94–104. http://dx.doi.org/10.1016/j.ress.2017.12.018.
[22] Der Kiureghian A, Liu PL. Structural reliability under incomplete probability information. J Eng Mech 1986;112(1):85–104. http://dx.doi.org/10.1061/(ASCE)0733-9399(1986)112:1(85).
[23] Nataf A. Détermination des distribution de probabilités dont les marges sont données. C R Acad Sci 1962;225:42–3.
[24] Lebrun R, Dutfoy A. An innovating analysis of the nataf transformation from the copula viewpoint. Probab Eng Mech 2009;24(3):312–20. http://dx.doi.org/10.1016/j.probengmech.2008.08.001.
[25] Grunwald C, Kaufmann M, Alter B, Vallée T, Tannert T. Numerical investigations and capacity prediction of g-frp rods glued into timber. Compos Struct 2018;202:47–59.
[26] Vallée T, Tannert T, Hehl S. Experimental and numerical investigations on full-scale adhesively bonded timber trusses. Mater Struct 2011;44(10):1745–58.
[27] Tannert T, Vallée T, Hehl S. Probabilistic strength prediction of adhesively bonded timber joints. Wood Sci Technol 2012;46(1):503–13.
[28] Grunwald C, Fecht S, Vallée T, Tannert T. Adhesively bonded timber joints–do defects matter? Int J Adhes Adhes 2014;55:12–7.
[29] Jiang C, Zhang W, Wang B, Han X. Structural reliability analysis using a copula-function-based evidence theory model. Comput Struct 2014;143:19–31.
[30] Zhou T, Peng Y. Structural reliability analysis via dimension reduction, adaptive sampling, and monte carlo simulation. Struct Multidiscip Optim 2020;62(5):2629–51.
[31] Blass HJ, Bienhaus A, Krämer V. Effective bending capacity of dowel-type fasteners. Proc PRO 2001;22:71–80.
[32] Thelandersson S, Larsen HJ. Timber engineering. John Wiley & Sons; 2003.
[33] Santos CL, De Jesus AMP, Morais JJL, Lousada JLPC. A comparison between the en 383 and astm d5764 test methods for dowel-bearing strength assessment of wood: Experimental and numerical investigations. Strain 2010;46(2):159–74. http://dx.doi.org/10.1111/j.1475-1305.2008.00570.x.

[34] Branco JM, Sousa HS, Lourenço PB. Experimental analysis of maritime pine and iroko single shear dowel-type connections. Constr Build Mater 2016;111:440–9. http://dx.doi.org/10.1016/j.conbuildmat.2016.02.134.
[35] Jorissen AJM. Double shear timber connections with dowel type fasteners. The Netherlands: Delft University Press Delft; 1998.
[36] Schmid M, Blaß HJ, Frasson RPM, distances Effectof. Effect of distances spacing and number of dowels in a row on the load carrying capacity of connections with dowels failing by splitting, in: Proceedings of the CIB W18 meeting, paper CIB-W18/31-9-1, kyoto, japan; 2002.
[37] Johansen KW. Theory of timber connections. Int Assoc Bridge Struct Eng 1949;9:249–62.
[38] Blaß HJ, Schädle P. Ductility aspects of reinforced and non-reinforced timber joints. Eng Struct 2011;33(11):3018–26.
[39] Shu Z, Li Z, Yu X, Zhang J, He M. Rotational performance of glulam bolted joints: Experimental investigation and analytical approach. Constr Build Mater 2019;213:675–95.
[40] Zhang C, Guo H, Jung K, Harris R, Chang W-S. Screw reinforcement on dowel-type moment-resisting connections with cracks. Constr Build Mater 2019;215:59–72.
[41] Jensen JL, Quenneville P. Fracture mechanics analysis of row shear failure in dowelled timber connections. Wood Sci Technol 2010;44(4):639–53.
[42] Yurrita M, Cabrero JM. New design model for splitting in timber connections with one row of fasteners loaded in the parallel-to-grain direction. Eng Struct 2020;223:111155.
[43] Rammer DR, Winistorfer SG. Effect of moisture content on dowel-bearing strength. Wood Fiber Sci 2007;33(1):126–39.
[44] Whale L, Smith I, Hilson BO. Behaviour of nailed and bolted joints under short-term lateral load - conclusion from recent research. In: Paper 19-7-1, proceedings CIB-W18 meeting. Florence, Italy; 1986.
[45] Whale L, Smith I. The derivation of design clauses for nailed and bolted joints in eurocode 5. In: Paper 19-7-6, proceedings CIB-W18 meeting. Florence, Italy; 1986.
[46] Whale L, Smith I, Larsen HJ. Design of nailed and bolted joints-proposals for the revisin of existing formular in draft eurocode 5 and the CIB code. In: Paper 20-7-1, proceedings CIB-W18 meeting. Dublin, Ireland; 1987.
[47] Eurocode 5: design of timber structures - part 1-1: general - common rules and rules for buildings. StandArd BS EN 1995-1-1, CEN – European Committee for StandArdization; 2014.
[48] Glišović I, Stevanović B, Kočetov-Mišulić T. Embedment test of wood for dowel-type fasteners. Wood Res 2012;57(4):639–50.
[49] Whale LRJ, Smith I. A method for measuring the embedding characteristics of wood and wood-based materials. Mater Struct 1989;22(6):403–10. http://dx.doi.org/10.1007/BF02472217.
[50] Sawata K, Yasumura M. Determination of embedding strength of wood for dowel-type fasteners. J Wood Sci 2002;48(2):138–46. http://dx.doi.org/10.1007/BF00767291.
[51] Franke S, Quenneville P. Investigation of the embedding strength of new zealand timber and view for the nz standard. In: Incorporating sustainable practice in mechanics and structures of materials. 2010, p. 897–902.
[52] NDS: national design specification for wood construction. StandArd BS EN 1995-1-1, American national standards institute and American forest & paper association; 2015.
[53] Tuhkanen E, Mölder J, Schickhofer G. Influence of number of layers on embedment strength of dowel-type connections for glulam and cross-laminated timber. Eng Struct 2018;176:361–8. http://dx.doi.org/10.1016/j.engstruct.2018.09.005.
[54] Timber structures: Test methods - determination of the yield moment of dowel type fasteners. Standard EN 409, CEN – European Committee for Standardization; 1993.
[55] Timber structures: joints made with mechanical fasteners - general principles for the determination of strength and deformation characteristics (ISO 6891:1983). Standard EN 26891, CEN – European Committee for Standardization; 1991.
[56] Werner H, Siebert W. Neue untersuchungen mit nägeln für den holzbau. Holz Als Roh-Und Werkst 1991;49(5):191–8.
[57] Blaß HJ, Colling F. Load-carrying capacity of dowelled connections, in: Proceedings of the 48th INTER meeting; 2015.
[58] Sandhaas C, Görlacher R. Analysis of nail properties for joint design. Eng Struct 2018;173:231–40.
[59] Timber structures: glued laminated timber and glued solid timber - requirements. Standard EN 14080, CEN – European Committee for Standardization; 2013.
[60] Cabrero JM, Yurrita M. Performance assessment of existing models to predict brittle failure modes of steel-to-timber connections loaded parallel-to-grain with dowel-type fasteners. Eng Struct 2018;171:895–910. http://dx.doi.org/10.1016/j.engstruct.2018.03.037.
[61] Elbashir D, Branco JM, Rodrigues LG. Reinforcement of dowel-type timber joints with self-tapping screws. Proc Inst Civ Eng-Struct Build 2020;173(12):969–88.
[62] Metallic materials - tensile testing - part 1: Method of test in ambient temerature. Standard EN 10002-1, CEN – European Committee for Standardization; 2001.
[63] Hot rolled products of structural steels. Technical delivery conditions for non-alloy structural steels. Standard EN 10025-2, CEN – European Committee for Standardization; 2019.
[64] Haldar A, Mahadevan S. Probability, reliability, and statistical methods in engineering design. John Wiley; 2000.
[65] Montgomery DC, Runger GC. Applied statistics and probability for engineers. John Wiley & Sons; 2018.
[66] Sakamoto Y, Ishiguro M, Kitagawa G. Akaike information criterion statistics, dordrecht. The Netherlands: D. Reidel; p. 81.
[67] Massey Jr FJ. The kolmogorov-smirnov test for goodness of fit. J Amer Statist Assoc 1951;46(253):68–78. http://dx.doi.org/10.1080/01621459.1951.10500769.
[68] Marelli S, Sudret B. UQLab: a framework for uncertainty quantification in MATLAB. In: Proc. 2nd int. conf. on vulnerability, risk analysis and management (ICVRAM2014). United Kingdom: Liverpool; 2014.
[69] Nelsen R. An introduction to copulas. Springer Science & Business Media; 2006.
[70] Sklar A. Fonctions de répartition à n dimensions et leurs marges, vol. 8. Publications de l'Institut de Statisque de L'Université; 1959, p. 229–31.
[71] Joe H. Dependence modeling with copulas. CRC Press; 2014.
[72] Kurz M. Vine copulas with matlab. https://github.com/MalteKurz/VineCopulaMatlab.
[73] Ang A, Tang W. Probability concepts in engineering planning and design, 2: Decision, risk, and reliability. John Wiley & Sons; 1984.
[74] Melchers R, Beck A. Structural reliability analysis and prediction. John Wiley & Sons; 2018.
[75] Gong J, Yi P. A robust iterative algorithm for structural reliability analysis. Struct Multidiscip Optim 2011;43(4):519–27. http://dx.doi.org/10.1007/s00158-010-0582-y.
[76] Galambos T, Ellingwood B, MacGregor J, Cornell C. Probability based load criteria: Assessment of current design practice. J Struct Div 1982;108(5):959–77.
[77] Honfi D, Mårtensson A, Thelandersson S. Reliability of beams according to eurocodes in serviceability limit state. Eng Struct 2012;35:48–54. http://dx.doi.org/10.1016/j.engstruct.2011.11.003.